Inorganica Chimica Acta, *134* (1987) 59–66

Magnetostructural Correlations in Parallel Square-planar Halo-bridged Copper(II) Dimers.

Part II: Structure and Magnetic Properties of $[Cu_2(terpy)_2Br_2](PF_6)_2$

TEOFILO ROJO*, MARIA I. ARRIORTUA, JOSE L. MESA, ROBERTO CORTES

Departamentos de Química y Cristalografía-Mineralogía, Facultad de Ciencias, Universidad del País Vasco, Apdo. 644, 48080 Bilbao, Spain

GERARD VILLENEUVE

Laboratoire de Chimie du Solide du C.N.R.S., 351 Cours de la Libération, 33405 Talence Cédex, France

and DANIEL BELTRAN

Departamento de Química Inorgánica, Facultad de Ciencias Químicas, Universidad de Valencia,, C/Dr. Moliner 50, 46100 Burjassot (Valencia), Spain

(Received February 19, 1987)

Abstract

The crystal and molecular structure of bis-μ-bromo-bis [(2,2′:6′,2″ - terpyridyl) copper (II)] bis (hexafluorophosphate) has been determined from three dimensional single-crystal X-ray diffraction data, collected by counter techniques. The blue crystals belong to the monoclinic system, space group $P2_1/a$, with four formula units in a unit cell of dimensions $a = 20.40(2)$, $b = 13.35(2)$, $c = 6.453(8)$ Å and $\beta = 97.74(9)°$. The structure was solved using a refinement procedure and starting with the atomic positions of the isostructural complex $[Cu(terpy)Cl]_2(PF_6)_2$, to final agreement factors $R = 0.071$ ($R_w = 0.077$). The structure consists of dimeric molecules bridged by two bromine atoms. The coordination geometry about the copper(II) ion is based on a distorted square pyramid with the bridging ligands occupying the apical and equatorial positions. The other three basal coordination positions are occupied by nitrogen atoms from the terpiridyl ligand. The apical Cu–Br bond distance is 2.83(9) Å, and the equatorial Cu–Br bond distance is 2.36(4) Å. The three copper–nitrogen bond lengths are 1.90(4), 2.01(4) and 2.01(8) Å. Both, magnetic susceptibility and ESR data evidenced the existence of exchange coupling. The best fit of the susceptibility data to the susceptibility expression for a pair of exchange coupled $S = 1/2$ ions leads to an evaluation of the singlet–triplet energy gap ($2J = -7.3$ cm^{-1}). A correlation is proposed relating the magnetic behaviour to the topology of the coordination polyhedron about the copper(II) ion in bis(μ-halo)-bridged parallel planar dimers.

Introduction

The interest of chemists and physicists, both experimentalists and theoreticians, in the study of the magnetic superexchange interactions has been manifested for several years. Nevertheless, at present, unfortunately, it is not yet possible to predict in a quantitative way the magnitude and kind of magnetic interactions, even for the simplest system, like the $S = 1/2$ dimers.

Nowadays, the study of correlations between the observed magnetic properties of a solid and its structural characteristics is the aim of intensive and systematic investigations [1]. For the simple case of copper(II) dimers both theoretical approaches and empirical correlations, particularly successful for di-μ-oxo bridged dimers [2], have been developed. However, the magnetic behaviour of halo-bridged copper dimers has been found to be more difficult to understand [1, 3].

Parallel planar copper(II) dimers are a special structural kind of complex where the magnetic interactions are expected to be always weak [4]. The role of out-of-plane copper–ligand interactions, the ligand nature and the metal environment topology are not well understood. The use of rigid quasi-planar ligands such as 2,2′,6′,2″-terpyridyl, give a relatively easy synthetic path to this kind of complex allowing the use of various bridging ligands [5, 6]. This work analyses the structure and magnetic properties of a bromide dimer within a general discussion on the magnetostructural correlations in the bis(μ-halo)-bridged parallel planar copper(II) dimers.

---

*Author to whom correspondence should be addressed.

0020-1693/87/$3.50

Experimental

Synthesis

Analytical grade copper(II) bromide, 2,2′:6′,2″-terpyridine (hereafter terpy) and potassium hexafluorophosphate were employed to prepare samples of $[Cu_2(terpy)_2Br_2](PF_6)_2$. An excess of a satured KPF_6 aqueous solution was added to a warm aqueous solution (20 ml) containing 0.4 g (0.768 mol) of the simple $Cu(terpy)Br_2$ complex [7]. The resulting solution was evaporated to obtain microcrystalline powder. Crystallization from a saturated aqueous solution of the latter precipitate gave blue needles of relatively good quality having the same composition and corresponding to the stoichiometry $[Cu(terpy)Br](PF_6)$. *Anal.* Calc. for $C_{15}H_{11}BrCuF_6N_3P$: C, 34.50; H, 2.10; N, 8.10; Cu, 12.20. Found: C, 34.50; H, 2.60; N, 8.30; Cu, 12.10%.

Structure Determination and Refinement

Weissenberg photographs taken with Cu Kα radiation showed systematic absences which implied that the space group is $P2_1/a$. Cell parameters are calculated from measurements on an automatic Phillips PW 1100 single diffractometer; $a = 20.40(2)$, $b = 13.35(2)$, $c = 6.453(8)$ Å, $\beta = 97.74(9)°$. Flotation of crystals in a bromoform–ethanol solution yielded $D_m = 2.08$ Mg m^{-3}, whereas the unit cell parameters give ($M = 521.4$ and $Z = 4$) $D_c = 1.99$ Mg m^{-3}. Intensity data were collected with graphite monochromated Mo Kα radiation using the ω–2θ scan technique in the range $3° < 2\theta < 25°$. From a total of 2088 reflections 798 were significantly ($I \geqslant 2.5\sigma(I)$) different from the background intensity. This intensity set was corrected for Lorentz and polarization effects. In the intensity reduction no correction was made for the crystal absorption in view of the small dimensions of the latter (0.80 × 0.05 × 0.04 mm). The structure was solved using a refinement procedure that began with the atomic position of the isostructural complex $[Cu(terpy)$-$[Cl](FP_6)$ [8], and was carried out by the computer program SHELX 76 with anisotropic thermal parameters to a final R value of 0.071 ($R_w = 0.077$, where $w = 1.6099/(\sigma^2[F_o] + 0.004697[F_o]^2)$.

Physical Measurements

Magnetic susceptibility measurements were performed on powdered samples in the temperature range 4.2 to 300 K using a Faraday type microbalance. All experimental data were corrected for diamagnetism and temperature independent paramagnetism, TIP (taken as -211.2×10^{-6} and 60×10^{-16} emu/Cu atom, respectively). A Brucker ER 200tt spectrometer equipped with a standard low-temperature device, operating at X-band calibrated by NMR probe for the magnetic field and a HP 5342A frequency counter for the microwave frequency, was used to record the EPR powder spectra of the complex at different temperatures. Visible reflectance spectra on solid powdered samples were recorded using a Cary 17 spectrometer. Infrared spectra on KBr discs were obtained from a Beckman 5260 spectrometer.

Results and Discussion

Description of the Structure

The structure of the bromine complex is very similar to that of the analogous chlorine complex [8]. The dimeric complex cation $[Cu_2(terpy)_2Br_2]^{2+}$, is built by two $[Cu(terpy)Br]^+$ units related through a molecular inversion center. A view of the dimeric entity is given in Fig. 1.

The final positional parameters for the non hydrogen atoms and the bond lengths and angles for the complex are given in Table I and Table II respectively.

Each copper ion is surrounded by a quasiplanar tridentate ligand (the mean Cu–N bond distance is 1.97 Å) and a bromine atom. The three nitrogen atoms of the terpy and the bromine one define a distorted square plane. The fifth coordination site (at the apical position) is occupied by a second bromine atom belonging to the other half of the dimer. The copper–apical bromine bond distance of 2.83(9) Å is longer than the copper–basal bromine bond distance of 2.36(4) Å. The copper(II) coordination can be described as (4 + 1) [9], or elongated square pyramidal. The bridging Cu_2Br_2 unit is constrained to be planar by the presence of the crystallographic inversion center in the middle of the dimer. The intradimeric copper–copper distance is 3.64(4) Å and the bridging Cu–Br′–Cu′ angle (ϕ) is 88.6(2)°. The geometry of the ligand molecule is similar to that observed in other complexes [10, 11] as well as the Cu–N and Cu–Br bond distances. In the cell the dimeric entities are separated from one another by 6.5 Å.

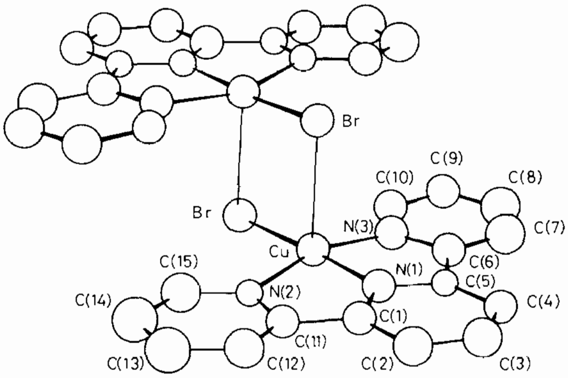

Fig. 1. View of the $[Cu_2(terpy)_2Br_2]^{2+}$ dimeric unit.

TABLE I. Positional Parameters and Equivalent Factors of Temperature[a]

Atom	x/a	y/b	z/c	B_{eq} (Å^2)[b]
Cu	0.0770(2)	0.0703(2)	0.0400(5)	3.74(1)
Br	0.0430(1)	−0.543(2)	−0.2110(4)	4.15(1)
P	0.3282(5)	0.0995(6)	0.1144(16)	4.89(2)
F(1)	0.3563(12)	0.2047(17)	0.1423(36)	11.89(5)
F(2)	0.3923(13)	0.0593(19)	0.2108(48)	15.28(6)
F(3)	0.2605(16)	0.1392(25)	0.0257(49)	15.99(5)
F(4)	0.3377(13)	0.0960(23)	−0.1065(42)	16.40(10)
F(5)	0.3105(15)	0.1111(25)	0.3363(40)	14.15(8)
F(6)	0.3007(14)	−0.0087(17)	0.0936(36)	12.98(7)
N(1)	0.1133(11)	0.1700(19)	0.2313(36)	3.73(2)
N(2)	0.0429(11)	0.1913(17)	−0.1255(42)	4.22(2)
N(3)	0.1330(11)	−0.0136(22)	0.2548(36)	4.20(3)
C(1)	0.0987(12)	0.2649(30)	0.1915(44)	4.59(4)
C(2)	0.1194(16)	0.3450(24)	0.3265(57)	5.37(3)
C(3)	0.1570(17)	0.3158(32)	0.5153(52)	5.99(4)
C(4)	0.1706(15)	0.2184(29)	0.5675(47)	5.09(3)
C(5)	0.1498(15)	0.1451(27)	0.4177(49)	4.18(3)
C(6)	0.1594(13)	0.0400(24)	0.4332(42)	3.89(3)
C(7)	0.1959(12)	−0.0056(29)	0.6043(41)	4.69(4)
C(8)	0.2031(14)	−0.1073(32)	0.6029(54)	5.64(5)
C(9)	0.1766(16)	−0.1651(29)	0.4326(66)	6.09(5)
C(10)	0.1417(14)	−0.1121(30)	0.2602(56)	5.66(5)
C(11)	0.0559(4)	0.2769(28)	−0.0191(45)	3.95(3)
C(12)	0.0332(16)	0.3697(26)	−0.1002(57)	5.30(3)
C(13)	−0.0086(17)	0.3700(28)	−0.3011(64)	6.02(3)
C(14)	−0.0214(16)	0.2845(33)	−0.4111(53)	5.38(3)
C(15)	0.0559(16)	0.1958(29)	−0.3270(56)	5.54(4)

[a]e.s.d.s in parentheses. [b]$B_{eq} = \frac{8}{3}\pi^2(U_{11} + U_{22} + U_{33})$.

The PF_6^- ion appears to be a regular octahedron with normal bond distances and angles as expected from the IR data (no splitting is observed for ν_3 and ν_4 infrared absorption bands which appear at 840 and 560 cm^{-1}, respectively). However, the high values of the fluorine thermal parameters (see Table I) indicate the existence of an important stirring of these atoms. These values have been found for other hexafluorophosphates [8, 12].

Electronic Spectroscopy and Magnetic Properties

The powder EPR spectrum of the complex exhibits a clear resolution of the g tensor in parallel and perpendicular components at room temperature ($g_\parallel$ = 2.204, $g_\perp$ = 2.049, $\bar{g}$ = 2.103, these values are slightly modified at 4 K, ($g_\parallel$ = 2.213, $g_\perp$ = 2.052, $\bar{g}$ = 2.108 (see Fig. 2). At temperatures below 60 K, a 'half field' signal has been observed that corresponds to forbidden $\Delta M_s = 2$ transitions which are characteristic of the presence of a magnetic exchange interaction between copper(II) pairs.

In the visible region, the complex exhibits an asymmetrical broad band centered at 15 100 cm^{-1}.

From the structural data, the symmetry of the $[CuN_3Br_2]$ chromophore is C_s and, consequently, an orthorhombic g tensor is expected. Nevertheless, from the experimental results, the o-rhombic component must be slight and, in order to interpret the spectroscopic data, an ideal C_{4v} symmetry is

TABLE II. Bond Lengths (Å) and Bond Angles (°)[a]

Cu–N(1)	1.90(4)	N(3)–C(10)	1.33(5)	C(13)–C(14)	1.35(6)
Cu–N(2)	2.01(4)	C(1)–C(2)	1.41(5)	C(14)–C(15)	1.39(6)
Cu–N(3)	2.01(8)	C(2)–C(3)	1.41(8)	C(1)–C(11)	1.52(8)
Cu–Br	2.36(4)	C(3)–C(4)	1.36(6)	C(5)–C(6)	1.42(5)
Cu–Br′	2.83(9)	C(4)–C(5)	1.40(5)	P–F(1)	1.52(2)
Cu–Cu′	3.64(4)	C(6)–C(7)	1.39(7)	P–F(2)	1.47(6)
N(1)–C(1)	1.32(5)	C(7)–C(8)	1.37(6)	P–F(3)	1.52(6)
N(1)–C(5)	1.37(7)	C(8)–C(9)	1.39(7)	P–F(4)	1.46(3)
N(2)–C(11)	1.34(4)	C(9)–C(10)	1.42(7)	P–F(5)	1.53(4)
N(2)–C(15)	1.41(8)	C(11)–C(12)	1.40(5)	P–F(6)	1.55(2)
N(3)–C(6)	1.40(5)	C(12)–C(13)	1.45(8)		
N(1)–Cu–N(2)	82(1)	C(14)–C(15)–N(2)	122(3)		
N(1)–Cu–N(3)	79(1)	N(3)–C(6)–C(7)	122(3)		
N(2)–Cu–Br	99(1)	C(7)–C(8)–C(9)	122(3)		
N(3)–Cu–Br	100(1)	C(9)–C(10)–N(3)	124(3)		
Br′–Cu–Br	91(0)	C(1)–C(2)–C(3)	114(3)		
Br′–Cu–N(1)	95(1)	C(3)–C(4)–C(5)	118(3)		
Br′–Cu–N(2)	91(1)	C(5)–N(1)–C(1)	119(3)		
Br′–Cu–N(3)	98(1)	C(11)–C(12)–C(13)	117(3)		
Cu–Br′–Cu′	89(0)	C(13)–C(14)–C(15)	118(3)		
N(1)–C(1)–C(2)	125(2)	C(15)–N(2)–C(11)	119(3)		
C(2)–C(3)–C(4)	123(3)	C(6)–C(7)–C(8)	118(3)		
C(4)–C(5)–N(1)	121(3)	C(8)–C(9)–C(10)	116(3)		
N(2)–C(11)–C(12)	122(3)	C(10)–N(3)–C(6)	117(2)		
C(12)–C(13)–C(14)	121(3)	N(2)–Cu–N(3)	160(1)		
N(1)–Cu–Br	174(1)				

[a]e.s.d.s in parentheses.

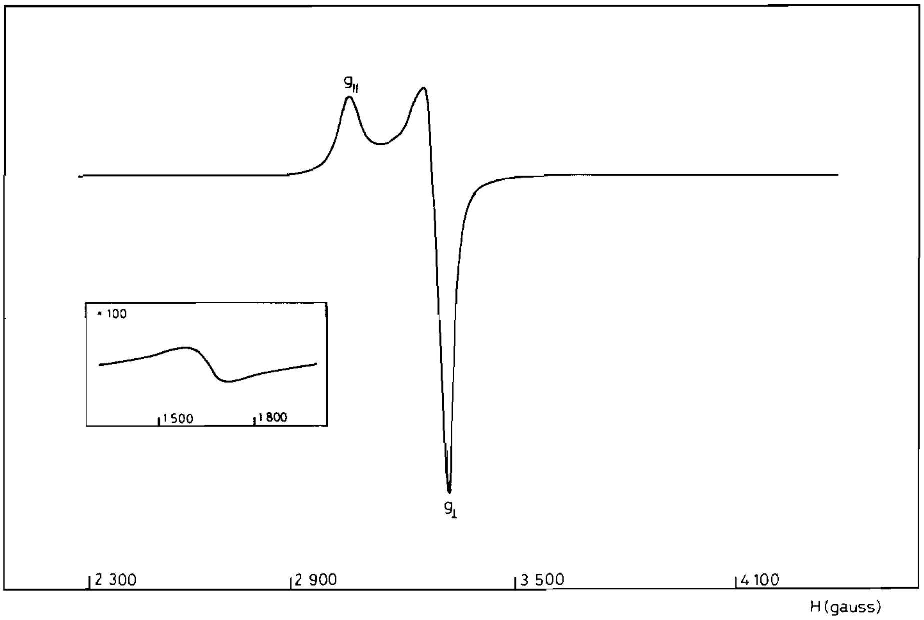

Fig. 2. X-band EPR spectrum of a powdered sample of $[Cu(terpy)Br]_2(PF_6)_2$.

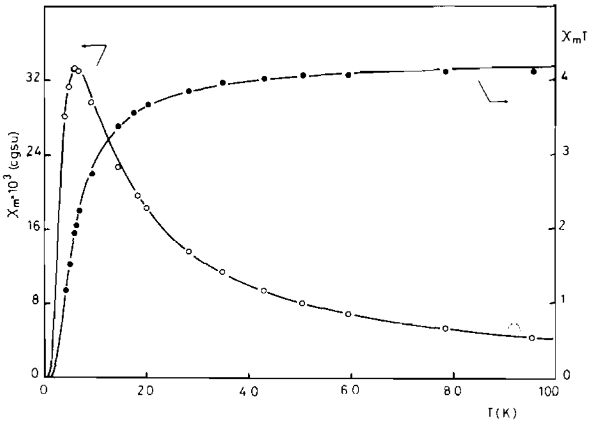

Fig. 3. Experimental molar paramagnetic susceptibility and effective magnetic moment for Cu^{2+} ion *vs.* temperature for the complex $[Cu(terpy)Br]_2(PF_6)_2$.

assumed. The observed trend of g values ($g_\parallel > g_\perp >$ 2.0023) is indicative of a $d_{x^2-y^2}$ ground state for the $[CuN_3Br_2]$ chromophore. A temperature assignment of the observed d–d transition is $B_1{}^2(d_{x^2-y^2}) \rightarrow {}^2B_2(d_{xy})$, ${}^2E(d_{xz,yz})$, $(\Delta_\parallel, \Delta_\perp)$, and, based on this assumption, it is possible to estimate the covalence factors from the orbital contributions using the expressions $g_\parallel = g_z = g_0 + 8u_\parallel$ and $g_\perp = g_{x,y} = g_0 + 2u_\perp$ (where $u = K_i{}^2\lambda_0/\Delta_i$ and $i = \parallel, \perp$; $\lambda_0 = 829$ cm^{-1}). The value obtained is $K = 0.67$, smaller than that calculated for the $[CuN_3Cl_2]$ chromophore in the analogous chlorobridged dimer [8], as expected for the substitution of the chlorine for the more polarizable bromine ligands.

The corrected molar susceptibility data are plotted *versus* the temperature in Fig. 3, that also includes the $\chi_m T$ values (the effective magnetic moment is defined as $(8\chi_M T)^{1/2}$ and the result of the fitting procedure). The magnetic susceptibility increases down to 6.3 K where a sharp maximum is defined and a brisk lowering of the $\chi_M T$ value is observed. It corresponds with a dropping of the effective moment from 1.80 BM at 300 K to 0.97 BM at 4.2 K.

The EPR data and the magnetic susceptibility behaviour indicate clearly the existence of a resultant antiferromagnetic intradimer coupling for this compound. The evaluation of the singlet–triplet energy splitting has been performed by a least-squares fit of the susceptibility data to the Bleaney–Bowers equation [13]. The best fitting provides an energy gap value of -7.3 cm^{-1} (-10.5 K). The $\bar{g}$ value was fixed to 2.103 from the EPR results.) The use of an isotropic Hamiltonian $\hat{\mathcal{H}} = -2J\hat{S}_1\hat{S}_2$ can be justified by an estimation of the values of the anisotropic exchange parameters J_d and D_d (antisymmetric exchange is absent owing to symmetry considerations), from the EPR variable temperature data on the 'half field' signal (J_d about 0.002 J). On the other hand, from the structural data the interdimeric distances are great (Cu–Cu *ca.* 6.5 Å; Cu–Cl *ca.* 5.3 Å) and, interdimeric magnetic interactions are expected to be negligible *versus* intradimeric ones at this range of temperatures.

Magnetostructural Correlations

In a previous paper [8]we have shown the correlation between the exchange energy (J) and the ratio

TABLE III. Distortion of the Coordination Polyhedron for the $[Cu(terpy)Br]_2^{2+}$ Compound and for the Ideal Geometries[a]

Designation	TBP	SP_{th}	SP_{tr}	$[Cu(terpy)Br]_2^{2+}$	SP
δa_1	101.5	106.4	109.9	116.1	121.8
δa_3	101.5	106.4	109.9	113.2	121.8
δa_4	101.5	106.4	109.9	119.9	121.8
δa_6	101.5	106.4	109.9	117.5	121.8
δa_2	101.5	93.0	88.0	78.7	73.9
δa_5	101.5	93.0	88.0	94.3	73.9
δe_1	53.1	55.5	64.1	67.3	73.9
δe_2	53.1	55.5	64.1	74.9	73.9
δe_3	53.1	46.6	28.7	1.5	0
	$\Delta = 0$	0.22	0.46	$\Delta = 0.75$	$\Delta = 1$

$$\Delta = \frac{[(\delta a_1 + \delta a_3 + \delta a_4 + \delta a_6) - 406.0]}{182.7} + \frac{[(\delta a_2 + \delta a_5) - 203.0]}{248.4} + \frac{[(\delta e_1 + \delta e_2) - 106.2]}{187.2} + \frac{[53.1 - \delta e_3]}{477.9}$$

[a] TBP, trigonal bipyramid; SP_{th}, tetrahedral distorted square pyramid; SP_{tr}, trigonal distorted square pyramid; SP, regular square pyramid.

$\alpha_1/2R$ (α_1 being *trans*-bridging angles and R the longer Cu–Cl′ distance) for several topologies of the bis(μ-chloro)-bridged parallel planar copper(II) dimers. At the same time, Landee and Greeney [14] carried out a similar study for bis(μ-halo)-bridged copper dimers utilizing only the *trans*-bridging angle values, and considering all complexes with tetragonal pyramidal geometry. In both cases, a better correlation than that observed by Hatfield and co-workers [15] between the exchange energy and the ratio ϕ/R (where ϕ is the bridging angle and R the long Cu–Cl′ distance) has been found.

We have quantified the distortions from the trigonal bipyramid (TBP, $\Delta = 0$) towards the tetrahedral distorted and trigonal distorted square pyramid [SP_{th} ($\Delta = 0.22$) and SP_{tr} ($\Delta = 0.46$), respectively] geometries described by Hathaway [9] (see Table III). This quantification has been realized using the model of Muetterties [16] and considering the regular square pyramid (SP) as the limit geometry. Based on this model, the distortion for the title compound has been calculated (see Table III). As expected, the value obtained $\Delta = 0.75$ shows a topology close to a regular square pyramid (SP). Likewise, other bis(μ-halo)-bridged copper(II) dimers that have been structurally and magnetically characterized are topologically classified in Table IV. In this quantitative classification there are some variations with respect to one previous qualitative classification established by us [8]. Thus, the $[Cu(tmen)Cl_2]_2$, $[Cu(2\text{-pic})Cl_2]_2$ and $[Cu(guaH)Cl_2]_2$ complexes with $\Delta = 0.87$, 0.63 and 0.30 deviations to TBP have now been classified as SP, SP_{tr} and SP_{th} geometries respectively. The $[Cu(4)\text{-}Meox)_2Cl_2]_2$ complex ($\Delta = 0.70$) shows an intermediate topology between the SP and SP_{tr} geometries. However, these results do not modify the conclusions of the preceding work significantly.

From the data presented in Table IV, it can be seen that the bromide dimers have a stronger antiferromagnetic coupling than the chloride analogues except for the TMEN and 2-PIC dimers which are not isostructurals. These values agree with the trend observed by Willett *et al.* [1] for the bromide and chloride salts. The complexes which are not isostructurals (DIEN dimers) show a ferromagnetic behaviour. As far as we know, all the considered dimers hold a symmetry centre except for $[Cu(dien)Cl]_2(ClO_4)_2$ in which the coordination polyhedron about each copper(II) ion shows a similar deviation from the trigonal bipyramid geometry ($\Delta Cu_1 = 0.83$; $\Delta Cu_2 = 0.91$). The dimers with a symmetry centre satisfy the expression $\phi/R = \alpha_1/2R + \delta/R$ relating the bridge angle to the angles that characterize the deviations of the actual dimer geometries in the

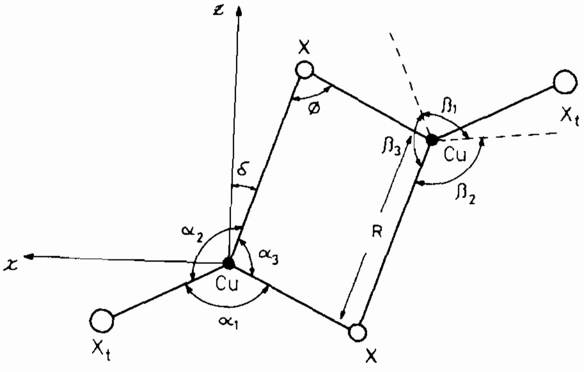

Fig. 4. Representation of the various angles considered in Table IV.

TABLE IV. Values of the Different Angles Considered in Fig. 4 for Various Copper(II) Dimers[a]

Dimer	R (Å)	α_1 (°)	α_2 (°)	α_3 (°)	β_1 (°)	β_2 (°)	β_3 (°)	$\alpha_1/2R$ (°) (Å)$^{-1}$	J (cm^{-1})	Δ	Geometry	Morphology	*trans* Ligand atom	Reference
1 $[Cu(dmen)Br_2]_2$	2.868	166.2	94.8	96.3	172.9	97.2	89.9	29.0	−1.2	0.78	SP	I	N	17
$[Cu(dmen)Cl_2]_2$	2.734	167.7	95.1	93.9	173.6	98.2	88.1	30.7	−1.05	0.80	SP		N	17
2 $[Cu(dmgH)Br_2]_2$	2.88	167.5	92.8	94.4	166.0	96.8	91.8	29.1	−1.5	0.88	SP	I	N	18, 19
$[Cu(dmgH)Cl_2]_2$	2.698	166.7	96.8	92.0	165.9	92.3	95.6	30.9	+3.15, 0.15	0.76	SP		N	19, 20
3 $[Cu(terpy)Br]_2(PF_6)_2$	2.83	173.9	94.7	91.4	159.0	97.5	90.7	30.7	−3.65	0.75	SP	I	N	this work
$[Cu(terpy)Cl]_2(PF_6)_2$	2.723	176.5	92.1	90.1	170.0	97.9	94.5	32.4	−2.95	0.81	SP		N	8
4 $[Cu(dien)Br]_2(ClO_4)_2$	2.887	178.8	89.5	89.4	160.6	100.7	96.0	31.0	+1.35	0.81	SP	NI	N	21
$[Cu(dien)Cl]_2(ClO_4)_2$	2.770	173.2	86.2	87.0	162.9	96.4	98.9	31.3	+0.2	0.83	SP		N	22, 23
	2.735	179.3	90.6	88.8	170.2	97.7	104.3	32.8		0.91				
5 $[Cu(tmen)Br_2]_2$	3.20	173.2	89.9	84.4	158.3	104.4	97.1	27.1	−2.0	0.87	SP	NI	N	24
$[Cu(tmen)Cl_2]_2$	3.147	170.8	88.4	83.2	157.5	105.9	96.4	27.1	−2.8	0.87	SP		N	25
6 $[Cu(2\text{-}pic)_2Br_2]_2$	3.872	176.2	96.6	79.6	176.2	92.9	91.0	22.8	−2.5	0.52	SP_{tr}	NI	Br	26
$[Cu(2\text{-}pic)_2Cl_2]_2$	3.364	177.6	98.2	79.2	173.4	91.8	94.8	26.4	−3.7	0.63	SP_{tr}		Cl	27, 28
7 $[Cu(4\text{-}meox)_2Br_2]_2$	2.71	157.2	109.9	93.0	172.7	94.1	93.0	29.0	−7.6	0.49	SP_{tr}	I	Br	29
$[Cu(4\text{-}meox)_2Cl_2]_2$	2.598	159.0	110.5	90.5	174.5	93.1	92.2	30.6	−1.3	0.70	SP		Cl	30
8 $[Cu(tmso)Br_2]_2$	2.981	139.6	94.5	125.9	169.9	84.8	91.3	23.4	−16.9	0.73	SP	I	Br	14
$[Cu(tmso)Cl_2]_2$	3.02	145.7	91.5	122.8	165.2	92.1	92.8	24.1	−8.5	0.50	PS_{tr}		Cl	31
9 $[Cu(4\text{-}metz)_2Br_2]_2$	3.033	171.9	102.0	85.8	169.2	96.4	94.4	28.3	−1.24	0.68	SP_{tr}		Br	32
10 $[Cu(maep)Br_2]_2$	2.802	172.8	86.5	87.9	141.6	122.2	95.8	30.8	−2.15	0.29	SP_{th}		N	33
11 $[Cu(guaH)Cl_2]_2$	2.447	168.7	86.7	82.1	111.7	114.3	134.0	34.5	−41.3	0.30	SP_{th}		Cl	34–38
12 $[Co(en)_3]_2[Cu_2Cl_8]Cl_2$	2.703	187.4	87.8	84.8	145.3	118.3	96.3	34.7	−7.3	0.28	SP_{th}		Cl	39–41
13 $[Cu(amp)Cl_2]_2$	2.862	172.5	93.7	89.3	170.6	92.4	88.6	30.1	−1.75	0.85	SP		N	42
14 $[Cu(Et_3en)Cl_2]_2$	2.728	185.1	91.0	85.2	145.7	111.0	103.0	33.9	+0.03	0.34	SP_{th}		N	15

[a] Abbreviations: dmen = *N,N*-dimethylethylenediamine; dmgH = dimethylglyoxime; terpy = 2,2′:6′,2″-terpyridine; dien = diethylenetriamine; tmen = *N,N,N′,N′*-tetramethylethylenediamine; 2-pic = 2-methylpyridine; 4-meox = 4-methyloxazole; tmso = tetramethylene sulfoxide; 4-metz = 4-methylthiazole; maep = 2-(2-methylamino)ethyl) pyridine; guaH = guaninium ion; en = ethylenediamine; amp = 2-aminomethylpyridine; Et_3en = *N,N,N′*-triethylethylenediamine. I = isostructural; NI = not isostructural; SP = regular square pyramid; SP_{tr} = trigonal distorted square pyramid; SP_{th} = tetrahedral distorted square pyramid geometries.

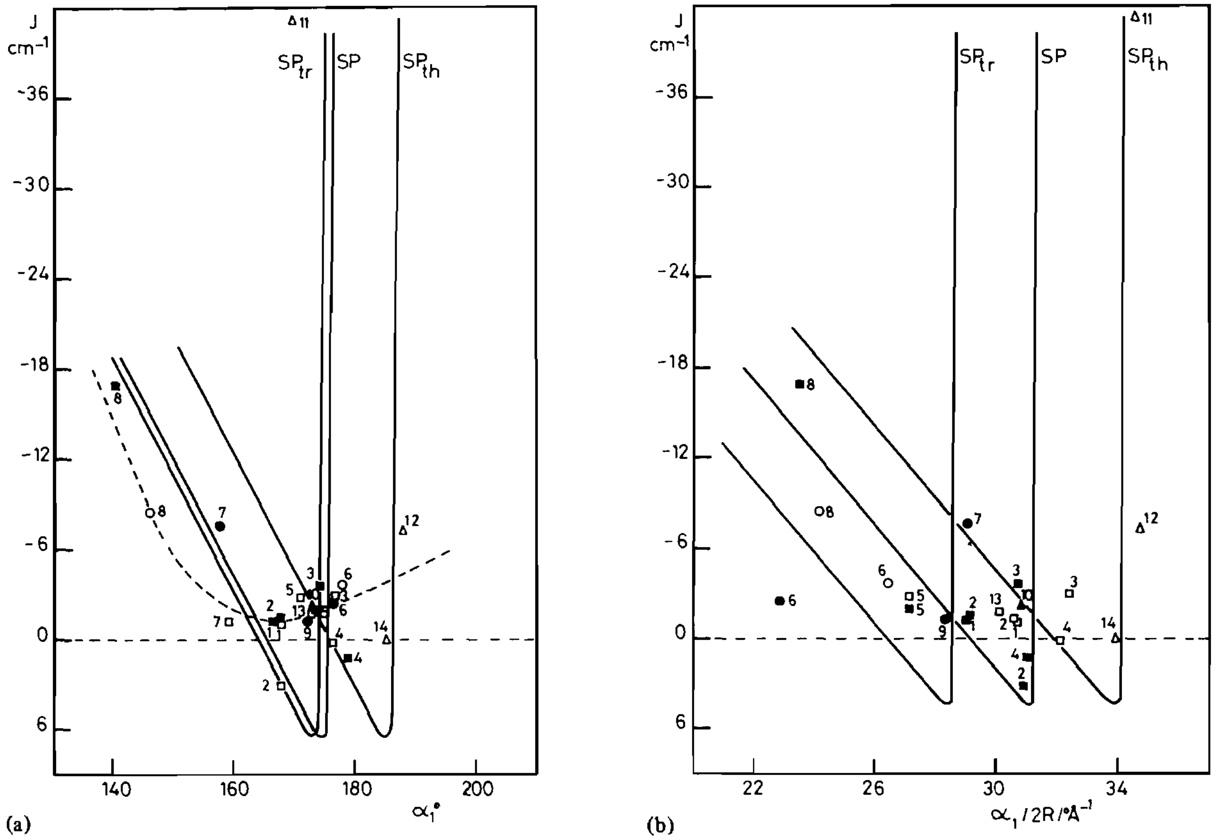

Fig. 5. Variation of the J parameter (a) *vs.* α_1 (the dashed curve gives the correlation suggested in ref. 14) and (b) *vs.* $\alpha_1/2R$ (see Table IV for the notations). ▪ = SP, ● = SP_{tr}, ▲ = SP_{th} and □ = SP, ○ = SP_{tr}, △ = SP_{th} geometries for the bromide and chloride compounds respectively.

bridge plane from those for an ideal square-planar dimer (see Fig. 4).

Plotting the exchange strengths (J) *versus* the *trans* X_t–Cu–X bridging angles (α_1) for both the bromide and chloride compounds of Table IV, it can be seen that the experimental values show certain correlations according to the topologies earlier described (see Fig. 5a), notwithstanding that the SP and SP_{tr} families lie very close and may be confounded (the dashed curve gives the correlation suggested by Landee and Greeney [14] considering all complexes with the same geometry). However, the best correlation for the three geometries is observed if the exchange energies (J) are plotted *versus* the ratio $\alpha_1/2R$ (see Fig. 5b). The curves show minima to approximate values of $\alpha_1/2R$ equal to 28, 31 and 34 $Å^{-1}$ for SP_{tr}, SP and SP_{th} geometries respectively, which will remain invariable. It therefore appears that the dominant factors controlling the superexchange strength in the parallel square-planar dimers are not related to the bridging angle but instead to the amount of distortion within the copper basal plane and to the distance of copper(II) to apical halogen in each topological family.

Likewise, it is important to note the influence of the nature of ligands *trans* to the bridging one (see Fig. 4 and Table IV). Generally the dimers having a halo ion as *trans* ligand show greater antiferromagnetic interaction than the dimers with aliphatic or aromatic amines as *trans* ligand. This observation agrees with the expected trend proposed by Hoffmann and co-workers [43] about the influence of the electronegativity of the substituents on superexchange interactions.

Supplementary Material

Anisotropic thermal parameters and structure factors for [Cu(terpy)Br](PF_6) are available from the authors on request.

Acknowledgement

This work was supported in part by a grant of the C.A.I.C.Y.T. which we gratefully acknowledge.

References

1 R. D. Willett, D. Gatteschi and O. Kahn, 'Magneto-Structural Correlations in Exchange Coupled Systems', Reidel, Dordrecht, 1985.
2 D. J. Hodgson, *Prog. Inorg. Chem., 19*, 173 (1975).
3 W. E. Hatfield, 'Theory and Application of Molecular Paramagnetism', Wiley, New York, 1976.
4 R. L. Lindvedt, M. D. Glick, B. K. Tomlonovic, D. P. Gavel and J. M. Kunszaj, *Inorg. Chem., 15*, 1633 (1976).
5 T. Rojo, *Ph.D. Thesis*, Universidad del País Vasco, 1981.
6 J. Ruiz, J. L. Mesa, M. I. Arriortua and T. Rojo, *J. Appl. Crystallogr., 16*, 430 (1983).
7 T. Rojo, J. L. Mesa, M. I. Arriortua and D. Beltran, *An. Quim, 80B*, 477 (1984).
8 T. Rojo, J. Darriet, J. M. Dance and D. Beltrán, *Inorg. Chim. Acta, 64*, L105 (1982); T. Rojo, M. I. Arriortua, J. Ruiz, J. Darriet, G. Villeneuve and D. Beltrán, *J. Chem. Soc., Dalton Trans.*, 285 (1987).
9 B. J. Hathaway, *Coord. Chem. Rev., 41*, 423 (1982).
10 T. Rojo, M. Vlasse and D. Beltrán, *Acta Crystallogr., Sect. C, 39*, 194 (1983).
11 M. Vlasse, T. Rojo and D. Beltrán, *Acta Crystallogr., Sect. C, 39*, 560 (1983).
12 M. I. Arriortua, T. Rojo, J. M. Amigó, G. Germain and J. P. Declerq, *Acta Crystallogr., Sect. B, 38*, 1323 (1982).
13 B. Bleaney and K. D. Bowers, *Proc. R. Soc. London, Ser. A, 214*, 451 (1952).
14 C. P. Landee and R. E. Greeney, *Inorg. Chem., 25*, 3771 (1986).
15 W. E. Marsh, K. C. Patel, W. E. Hatfield and D. J. Hodgson, *Inorg. Chem., 22*, 511 (1983).
16 E. L. Muetterties and L. J. Guggenberger, *J. Am. Chem. Soc., 96*, 1748 (1974).
17 D. W. Phelps, W. H. Goodman and D. J. Hodgson, *Inorg. Chem., 15*, 2266 (1976).
18 H. Endres, *Acta Crystallogr., Sect. B, 34*, 3736 (1978).
19 M. Megnamisi-Belombe and M. A. Novotny, *Inorg. Chem., 19*, 2470 (1980).
20 D. H. Svedung, *Acta Chem. Scand., 23*, 2865 (1969).
21 D. K. Towle, S. K. Hoffmann, W. E. Hatfield, P. Singh, P. Chaudhuri and K. Wieghardt, *Inorg. Chem., 24*, 4393 (1985).
22 S. K. Hoffmann, D. K. Towle, W. E. Hatfield, P. Chaudhuri and K. Wieghardt, *Inorg. Chem., 24*, 1307 (1985).
23 S. K. Hoffmann, D. K. Towle, W. E. Hatfield, K. Wieghardt, P. Chaudhuri and J. Weiss, *Mol. Cryst. Liq. Cryst., 107*, 161 (1984).
24 E. Luukkonen and A. Pajunen, *Suomen Kemi., B, 46*, 292 (1973).
25 E. D. Estes and W. E. Hatfield, *Inorg. Chem., 14*, 106 (1975).
26 P. Singh, D. Y. Jeter, W. E. Hatfield and D. J. Hodgson, *Inorg. Chem., 11*, 1657 (1972).
27 W. E. Marsh, W. E. Hatfield and D. J. Hodgson, *Inorg. Chem., 21*, 2679 (1982).
28 W. F. Duckworth and N. C. Stephenson, *Acta Crystallogr., Sect. B, 25*, 1969 (1975).
29 W. E. Marsh, T. L. Bowman, W. E. Hatfield and D. J. Hodgson, *Inorg. Chim. Acta, 59*, 19 (1982).
30 W. E. Marsh, D. S. Eggleston, W. E. Hatfield and D. J. Hodgson, *Inorg. Chim. Acta, 70*, 137 (1983).
31 D. D. Swank, G. F. Needdham and R. D. Willet, *Inorg. Chem., 18*, 761 (1979).
32 W. E. Marsh, T. L. Bowman, C. S. Harris, W. E. Hatfield and D. J. Hodgson, *Inorg. Chem., 20*, 3864 (1981).
33 R. B. Wilson, W. E. Hatfield and D. J. Hodgson, *Inorg. Chem., 15*, 1712 (1976).
34 J. A. Carrabine and M. Sundaralingam, *J. Am. Chem. Soc., 92*, 369 (1970).
35 J. P. Declercq, M. Debboudt and M. Van Meersche, *Bull. Soc. Chem. Belg., 80*, 527 (1971).
36 M. Sundaralingam and J. A. Carrabine, *J. Mol. Biol., 61*, 287 (1971).
37 R. F. Drake, V. H. Crawford, N. W. Laney and W. E. Hatfield, *Inorg. Chem., 13*, 1246 (1974).
38 J. F. Villa, *Inorg. Chem., 12*, 2054 (1973).
39 D. J. Hodgson, P. K. Hale and W. E. Hatfield, *Inorg. Chem., 10*, 1061 (1971).
40 J. A. Barnes, W. E. Hatfield and D. J. Hodgson, *Chem. Phys. Lett., 7*, 374 (1970).
41 K. T. McGregor, D. B. Losee, D. J. Hodgson and W. E. Hatfield, *Inorg. Chem., 13*, 756 (1974).
42 C. J. O'Connor, E. E. Eduok, J. W. Owens, E. E. Stevens and C. L. Klein, *Inorg. Chim. Acta, 117*, 175 (1986).
43 P. J. Hay, J. C. Thibeault and R. Hoffmann, *J. Am. Chem. Soc., 97*, 4884 (1975).